

Characterization of Bael Shell (*Aegle marmelos*) Pyrolytic Biochar



Monoj Bardalai and D. K. Mahanta

Abstract Biochar is found to be an important tool in improving the soil quality for agriculture. In this work, biochar was derived from *Aegle marmelos* (commonly known as bael) shell (AMS) by pyrolysis for evaluation and analysis of different properties. In the experiment of pyrolysis, a fixed bed reactor was used for the production of biochar from AMS. The range of particle size of the biomass feedstock was 0.5–1.0 mm, while pyrolysis temperature was fixed at 450 °C with the rate of heating as 15 °C/min. The heating value of the AMS biochar (i.e., 24.91 MJ/kg) is found to be higher when compared with the raw AMS (i.e., 18.11 MJ/kg). Thermogravimetric (TGA) and derivative thermogravimetric (DTG) analyses show that biochar decomposes at higher temperature due to the significant contamination of lignin. The surface morphology of AMS biochar reveals few small pores (e.g., 0.88–1.4 μm), and the surface area of the biochar according to Brunauer, Emmett, and Teller (BET) was measured to be low, i.e., 3.9 m²/g. The AMS biochar shows the pH value to be quite high as 9.3. The spectrum of Fourier transform infrared (FTIR) of the biochar indicates the presence of some compounds of aromatic functional groups with C=C stretching. The alkaline biochar of AMS becomes useful for the improvement of soil of acidic nature. Further, aromatic functional groups of AMS biochar enhance the soil stability.

Keywords *Aegle marmelos* · Biochar · Pyrolysis · Morphology · Soil

M. Bardalai (✉)

Department of Mechanical Engineering, Tezpur University, Tezpur 784028, India

e-mail: monojtezu@gmail.com

D. K. Mahanta

Department of Mechanical Engineering, AEC, Gauhati University, Guwahati 781013, India

© The Author(s), under exclusive license to Springer Nature Singapore Pte Ltd. 2021

R. M. Singari et al. (eds.), *Advances in Manufacturing and Industrial Engineering*,

Lecture Notes in Mechanical Engineering,

https://doi.org/10.1007/978-981-15-8542-5_65

1 Introduction

Biomasses are found almost every part of the world and considered as wastes. A major part of the biomass can be used as the substituting agent for soil fertilization. However, conversion of biomass into liquid and gaseous fuel and chemicals are the major concerns of the recent research. Although many conversion techniques are available, the pyrolysis and gasification are the most common and easy to perform [1]. In the process of pyrolysis, the feedstock is generally put inside a reactor in the temperature range of 400–700 °C in an environment of limited oxygen. During pyrolysis, the biomass undergoes many chemical reactions leading to convert the biomass into liquid (tar or pyrolytic oil), solid (biochar), and gas (incondensable gas). It is found that the properties of pyrolysis products such as biochar show better quality in comparison with the raw biomass. Therefore, biochar can be utilized as an agent for the improvement of soil properties [2, 3]. Although pyrolysis is mostly carried out to produce bio-oil, a significant amount of biomass (approximately 15–20%) is found to be solid product, i.e., biochar [4]. The biochar obtained by pyrolysis contains the residual of carbonaceous substance and can be the cause of natural fire with negligible amount of oxygen [5]. Biochar can also be used for the purpose of fertilization of soil, plant growth, decontamination of adulterant such as acaricides, heavy metallic substance, and compounds of hydrocarbon [6, 7].

In the past years, the use of biochar has been found as a substance for improvement and reclusion of C in soil [8]. Biochar can be considered as a by-product of pyrolysis in solid state, which is available in the form of black carbon with the presence of elemental carbon or graphite to aromatic carbon [9]. In general, biochar has much smaller specific area and micropore volume than the carbon which is activated commercially. However, the capacity of adsorption relative to organic pollutants and heavy metals are equivalent to and sometimes higher in comparison with the activated carbon [9]. Moreover, the detail study of the previous publications reveals that the biochar is useful for upgradation of soil properties, improving the productivity of crop, fixation of CO₂, and absorption of unnecessary ingredients [10]. Biochar is relatively stable in comparison with some other organic substances and sustainable for a long period of time in soil [11–13]. Further, the biochar has the ability of reduction of the release of major greenhouse gases such as CH₄ and N₂O, particularly from the soil of rice paddy field [14–16].

The variation of biochar in terms of physiochemical properties is influenced by the nature of biomass and conditions of pyrolysis experiment. In particular, the temperature used in pyrolysis process has the significant effects on the yield of biochar and its properties. It was observed that by increasing temperature in pyrolysis process, the yield of biochar is found to be decreased and at higher temperature, the biochar losses carbon, some important functional groups and development of useful microstructure [17, 18]. The pyrolysis temperature also affects the properties such as thermal stability, pH value, morphology of surface, and chemical composition [19].

Gottipatti and Mishra [20] used *Aegle marmelos* fruit shell in order to prepare microporous activated carbon (MAC) by KOH activation. This study was concentrated mainly on the porous characteristics of the activated carbon, such as pore volume, surface area, and pore size distribution. The same biomass was taken for the production of microporous activated carbon by activating $ZnCl_2$, and this MAC was applied for the removal of Cr (VI) from the aqueous solution [21]. Another study performed by Ahmed and Kumar [22] showed the possible application of AMS carbon as an absorbent to eliminate the congo red dye from aqueous solution. Roy et al. [23] performed the research on characterization and application of bael shell biochar in the removal of Patent Blue dye solution. Recently, Palniandy et al. [24] have studied the application of bio-char derived from different biomasses such as rubberwood and rice husk as fuel source in direct carbon fuel cells (DCFC) for power generation. However, the detail investigation of different properties of the pyrolyzed biochar of AMS dust is not much available in the previous publications. Although the bael tree is found in different parts of the world, it is abundantly available in the northeastern region of India. The inner part of bael fruit is very useful as food for various medicinal purposes. On the other hand, the outer part, i.e., the shell of the fruit is treated as waste. The biochar has many properties which are helpful in the improvement of soil quality for agricultural purposes such as plant nutrition. In order to reduce the wastes and to explore the properties of biochar, the bael shell was taken in the present study as the raw material for biochar production. The present work is concentrated on the production of AMS biochar by the process of pyrolysis and to characterize all the physiochemical properties with a detailed comparative study.

2 Materials and Methods

The AMS biochar was obtained as a solid product during the production of pyrolysis oil from AMS dust as explained by Bardalai and Mahanta [25]. Pyrolysis was carried out with a heating rate of $15\text{ }^\circ\text{C}/\text{min}$ in the range of temperature $450\text{--}600\text{ }^\circ\text{C}$. However, the biochar sample produced at $450\text{ }^\circ\text{C}$ was considered for various analyses at which the yield of biochar was about 45 wt%.

The proximate analysis, elemental analysis, TGA, FTIR, and pH measurement were carried out according to the methodology used in the previous publication [25]. For pH measurement, a mixture of biochar and deionized water was prepared in the ratio 1:20 (w/v) in order to obtain a homogeneous suspension to evaluate the pH value within 1.5 h. An analytical instrument was used to perform the crystallographic study known as XRD diffractometer (RIGAKU Mini flex, Japan). The operating voltage of XRD diffractometer was 30 kV while current density was 15 mA. The range of scanning was set at $2\theta = 10^\circ\text{--}70^\circ$, and the scanning speed was $0.05^\circ/\text{s}$.

The morphology study of the biochar surface was conducted with the help of scanning electron microscope—SEM (JEOL, JSM 6390 LV). BET (QUANTACHROME, NOVA 1000E) was used to measure the specific surface area (SSA) of biochar at

350.35 °C using N₂ sorption data. The timing of outgassing analysis was 6 h with the temperature of 100 °C.

For characterization of all physical and chemical properties of AMS biochar, the experiments were carried out for three times (standard deviation 0.5–1.5) and the average values of these results are tabulated in this paper.

3 Results and Discussion

Different analyses for AMS biochar were carried out and the results are presented in Table 1 and discussed in the following sections.

3.1 Proximate and Ultimate Analysis

The moisture content in AMS biochar is reasonably lower (refer Table 1) than the biomass as it was removed during pyrolysis process and found to be consistent with EFB biochar [26]. However, AMS biochar contains relatively higher moisture content when compared with the biochar obtained from coconut shell (CSB) and mesquite wood (MWB) as reported in Table 1 [27]. It can be seen that fixed carbon has increased by an amount of 60.87 wt% when AMS was converted into biochar indicating that the biochar is more carbonaceous than biomass and thus suitable for soil amendment. The fixed carbon in AMS biochar is found to be quite comparable with other biochar as seen in Table 1. High value of fixed carbon content helps the biochar in improving soil properties. During pyrolysis, a series of thermochemical reactions take place

Table 1 Proximate and ultimate analysis of AMS and AMS biochar

Property	AMS	AMS biochar	Other biochar
Moisture (wt%)	10.88	5.42	0.35–5.15 [26, 29, 32]
Volatile matter (dry basis, wt%)	90.56	29.82	7.2–17.62 [26, 29]
Fixed carbon (dry basis, wt%)	5.46	66.33	65.4–72.94 [26, 29]
Ash (dry basis, wt%)	3.98	3.00	7.9–67 [8, 26, 28, 29]
Calorific value (MJ/kg)	18.11	24.91	26.6–28.8 [33]
C (wt%)	41.80	70.87	22.5–74.19 [8, 26, 28, 29]
H (wt%)	5.80	3.99	1.6–3.48 [26, 28, 33]
N (wt%)	2.10	1.14	6.83 [26]
O (calculated by difference, wt%)	50.30	24	23.9–24.6 [26, 28]
H/C	1.67	0.68	0.62 [28]
O/C	0.90	0.25	0.27 [28]
pH	–	9.3	7.2–10.9 [8, 27–29, 34, 35]

leading to produce carbonaceous hydrocarbons from the oxygenated compounds and thus content of oxygen is found to be decreased in biochar. The amount of ash content in AMS biochar is significantly lower in comparison with many biochar which was obtained from the biomasses such as bamboo shoot shell (BSS) [28], palm empty fruit bunch (EFB) [26], and palm kernel shell (PKS) [29] as listed in Table 1. The biochar which contains low ash is preferred for the purpose of soil improvement, since the possibility of the presence of contaminants of heavy metallic compounds in ash is high and leads to pollute the soil [30]. Moreover, the biochar containing low ash content carries high calorific value, because the high ash content is responsible for diluting the energy value of the biochar [31]. In this study, it is seen that percentage of ash in AMS biochar is slightly more when compared with CSB and MWB as they ranged within 1.29–1.46 wt% [32].

Due to high carbon content, low ash, and oxygen content, the heating value of AMS biochar is relatively higher when compared with biomass (refer Table 1). The amount of carbon content in the present biochar is higher in comparison with the biochar obtained from sewage sludge (SS), municipal waste (MW), cattle digestate (CD), poultry litter (PL), BSS, and EFB [8, 26, 28]. However, the carbon content in AMS biochar is relatively lower than the biochar of PKS and cashew nutshell (CNS) produced at 450 °C [29, 33]. The calorific value of AMS biochar is relatively lower in comparison with CNS biochar due to lower carbon content [33].

The pH value of AMS biochar (see Table 1) can be compared with many biochar which are available in a significant number of publications. It is found that, pH of AMS biochar is higher when compared with the biochar of SS (pH = 7.2), MW (pH = 7.4), CSB (pH = 8.66), and MWB (pH = 8.73) [8, 32]. However, in AMS biochar, the pH value is slightly lower relative to the biochar produced from rice straw (RS), BSS, PKS, and argan shells (AS) [27–29, 34, 35]. The highly alkaline behavior of the biochar is found to be favorable for improving acidic soil.

The atomic ratios, i.e., O/C and H/C of AMS biochar, are significantly lower in comparison with raw AMS (Table 1). The reason of lower atomic ratios is the liberation of H and O at the time of pyrolysis relative to carbon according to the explanation of previous publications [27, 34–36]. The biochar with low value of H/C is highly aromatic. The highly aromatic biochar resists the decomposition and remains intractable, which is helpful in sequestering the carbon in soil [17, 37]. However, the atomic ratio, O/C of AMS biochar is higher in comparison with the biochar of wheat residue and activated carbon (e.g., 0.06–0.09). This reveals that biochar of AMS is highly hydrophilic due to the presence of more polar groups [9]. Further, in AMS biochar, H/C ratio is slightly higher and O/C ratio is lower when compared with BSS biochar indicating the release of higher amount of hydrogen and lower amount of oxygen relative to carbon [31]. These differences of atomic ratios are supposed to be due to polymerization of dehydrogenative radicals and dehydrating polycondensation at the time of pyrolysis [38].

3.2 Thermal Degradation Analysis

TGA profile of AMS dust (Fig. 1a) indicates that about 70 wt% of biomasses have decomposed in temperature range of 450–500 °C. The highest decomposition rate of AMS is observed at 259 °C as shown by DTG profile (Fig. 1a). This thermal behavior of AMS biomass is consistent with other biomasses, such as in CNS, where about 60 wt% degradation was observed in nitrogen atmosphere in the temperatures between 450 and 500 °C, while the decomposition rate was found to be highest at 300 °C [33]. Further, about 70% weight loss was observed upto 450 °C when EFB was thermally degraded and the highest rate of decomposition was at 300 °C [26]. Thus, the decomposition of AMS within the temperature of 450–500 °C is found to be quite similar to the other biomasses, and hence, the pyrolytic temperature for AMS was fixed at 450 °C. As the pyrolysis temperature increases, the lignin components start decomposing leading to the formation of tar which enhances in partially blocking the pores on biochar surface [39].

The TGA curve of AMS biochar (Fig. 1b) shows that about 3% till 100 °C followed by about 2% upto 300 °C mass loss has occurred. This is due to the release of physisorbed water. According to the TGA curve (Fig. 1b), significant degradation of the biochar starts from 300 °C, which reveals the degradation of lignin and residual cellulose available in the biochar. The DTG plot of AMS continues to rise upto about 450 °C, which represents the degradation of residual cellulose and lignin content [40]. The peak at around 448 °C on the DTG curve (Fig. 1b) indicates the highest rate of lignin and cellulose decomposition present in the biochar. Thus, the biochar derived from AMS with lignin content is useful for the promotion of *Fusarium oxysporum cucumerinum* (*f.o.c.*) survival in soil by growing the peculiar fungal flora [41].

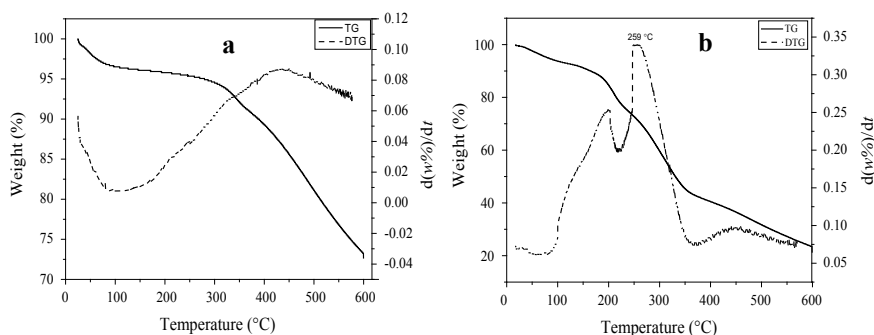


Fig. 1 Profiles of TGA and DTG for **a** AMS dust and **b** AMS biochar

3.3 FTIR Analysis

The peaks observed in the FTIR spectra of AMS and AMS biochar (Fig. 2) have been used in order to identify the functional groups of various compounds. A broad-band which centered near 3414 cm^{-1} is assigned to $-\text{OH}$ functional group in AMS. However, intensity of this peak is less when compared with the spectra of AMS biochar indicating the deterioration of hydroxyl compounds during conversion of biomass to biochar. The peaks at near to 2927 cm^{-1} are due to the presence of alkane group with $\text{C}-\text{H}$ stretching vibration which are found on both biomass and biochar. Similar type of functional group was identified in the FTIR spectrum of MWB biochar [32]. Few peaks in the band of 1600 and 1800 cm^{-1} in the spectrum as seen in Fig. 2 indicate the existence of functional groups of the compounds of alkanes, carbonyl ($\text{C}=\text{O}$), water, and oxygenated hydrocarbon with plane bending $-\text{OH}$, which disappear in AMS biochar [40]. This is the indication of reduction of oxygenated compounds from biomass to biochar. The intense peak near 1592 cm^{-1} with stretching vibration represents the ring bonding of aromatic and alkynes ($\text{C}\equiv\text{C}$) characteristic in the AMS biochar similar to MWB [32], which is not found in the raw AMS. Pituello et al. [8] also found the aromatic functional groups in the silage digestate biochar spectrum. The carbon-carbon double-bonded stretching aromatic peak reveals the presence of the ring of aromatic compounds such as benzene in the AMS biochar, which helps in stabilizing the soil. The strong peak of AMS spectrum at 1031 cm^{-1} indicates the stretching bond of $\text{C}-\text{C}-\text{O}$ or $\text{C}-\text{O}-\text{C}$, which are not significant in the spectrum of AMS biochar. Further, the peaks found within the band $500\text{--}700\text{ cm}^{-1}$ in AMS spectrum (centered at 611 cm^{-1}) is supposed to be hydroxyl group in the mode of out plane bending [40]. In FTIR spectrum of AMS biochar, the appearance of peak nearby 827 cm^{-1} is the agreement of the presence of aromatic functional group. This can be attributed to aromatic $\text{C}-\text{H}$ group which is to

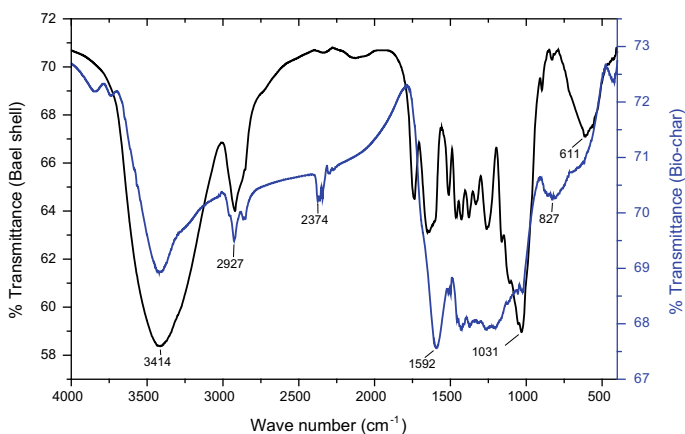


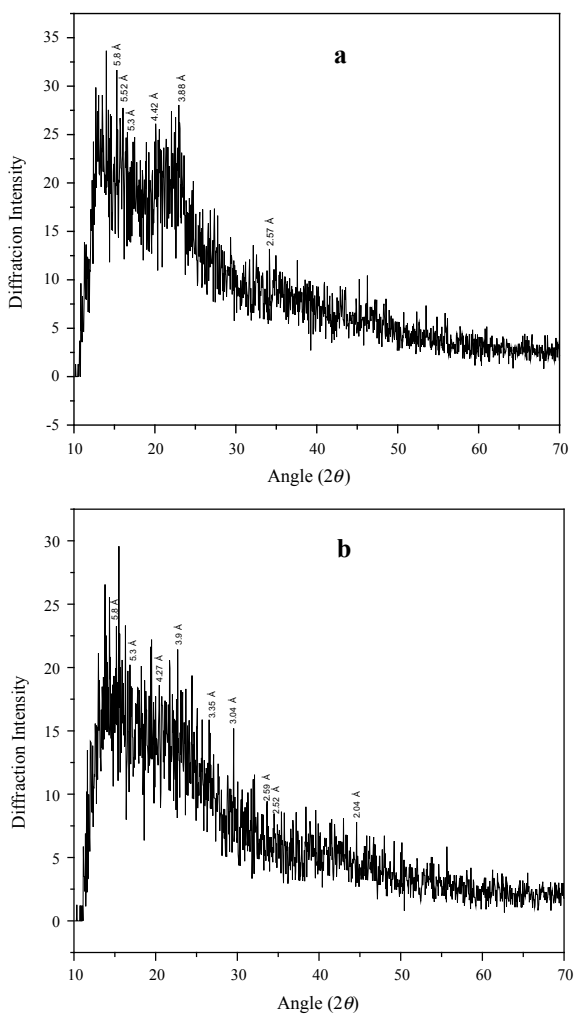
Fig. 2 FTIR spectra of AMS and AMS biochar

be out of plane deformation [32, 42, 43]. Thus, the FTIR analysis indicates that AMS consists of compound of oxygenated hydrocarbons, while aromaticity dominates the characteristics of AMS biochar.

3.4 Crystallographic Analysis

The XRD diffractograms of AMS and the AMS biochar are shown in Fig. 3a and b, respectively, where both the spectra clearly show the amorphous behavior. However, the peak spacings observed at 5.8 Å, 5.52 Å, 5.3 Å, 4.42 Å, 3.88 Å, 2.57 Å in Fig. 3a

Fig. 3 X-ray diffractograms of **a** AMS and **b** AMS biochar



indicate the crystal structure of cellulose in AMS [4, 19, 44]. This is due to the fact that cellulose in biomass may consist of a wide range of segments, which contain both amorphous and crystalline portions [45]. The peaks observed at 5.8 Å, 5.3 Å, 3.9 Å, 2.59 Å, and 2.52 Å in the diffractogram (Fig. 3b) of AMS biochar represent the crystalline structure of cellulose [19, 42]. The presence of SiO₂ in AMS biochar can be expected by the peaks at 4.27 Å and 3.35 Å (Fig. 3b) which is consistent with RS biochar [34]. Further, the possibility of calcite (CaCO₃) contamination in AMS biochar is detected by the peak identified at 3.04 Å [34]. The calcite content in biochar improves the soil of acidic nature and makes it useful for agricultural purposes. The presence of graphitic structure in the biochar of AMS can be explored by the peaks at the spacings of 3.35 Å and 2.04 Å [46].

3.5 Morphology Study

The SEM images of AMS biochar are shown with the magnifications 500×, 2500×, and 5500× in Fig. 4a–d, respectively. At low magnifications (Fig. 4a, b), the micrographs show no defined morphology which are similar to CNS biochar [33]. However, a few numbers of pores with diameter in the range of 0.51–1.40 μm are observed on the biochar surface (Fig. 4c, d). Therefore, the SSA of the biochar recorded by BET is found to be very low (3.9 m²/g). The SSA of AMS biochar is quite comparable with the results published by Shariff et al. [26], i.e., 0.1301–7.9890 m²/g. As the pyrolysis was carried out at low temperature, the surface area of AMS biochar was found to be relatively low [46]. The ash content and its composition are responsible for the occurrence of pores on the biochar surface. Inorganic compounds present in biochar such as ash and leads to plug the pores caused by pyrolysis [31, 47]. The less porosity on the biochar surface is also the result of the production of tar in pyrolysis which mixes with the biochar and tends to plug the pores. Few fibrillar structures can be seen in Fig. 4b, c, which is the indication of the presence of cellulose on AMS biochar and consistent with the results obtained in thermal and crystallographic analyses [8, 40].

The isotherms obtained in adsorption and desorption of nitrogen in AMS biochar reveal the growth of micropores on the biochar (Fig. 5). The volume of adsorption and desorption is not much significant at low relative pressure (e.g., 0.9), but becomes very high beyond that. At low relative pressure, desorption is higher than adsorption, while at higher relative pressure, both adsorption and desorption curves coincide and good agreement of the study carried out by some previous researchers with the analysis gas CO₂ and N₂ [40, 46]. This study reveals the partial desorption of nitrogen in the AMS biochar.

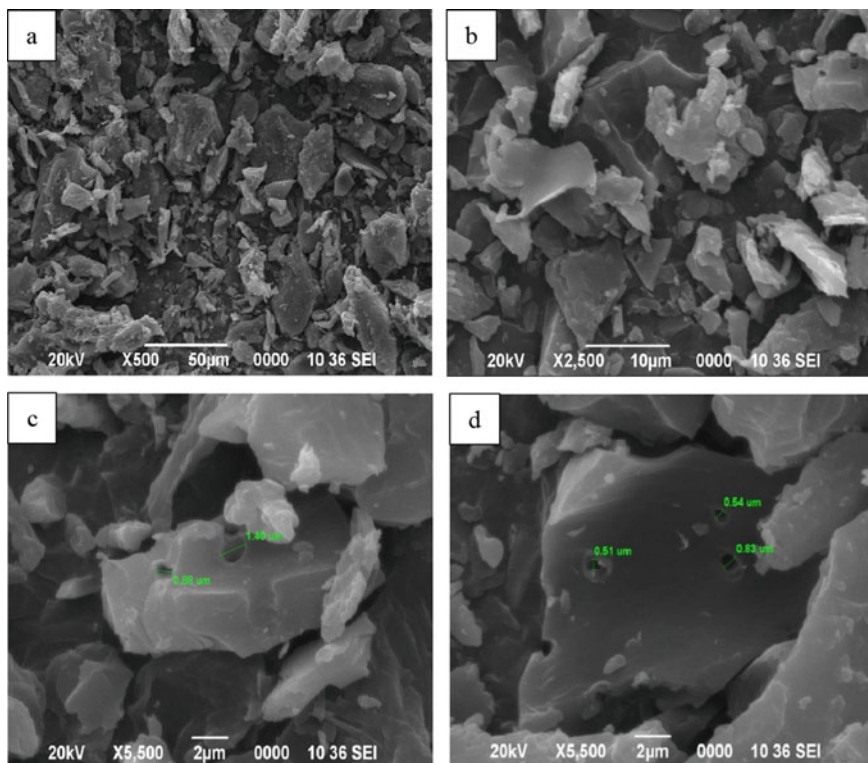


Fig. 4 SEM images of AMS biochar at various magnifications

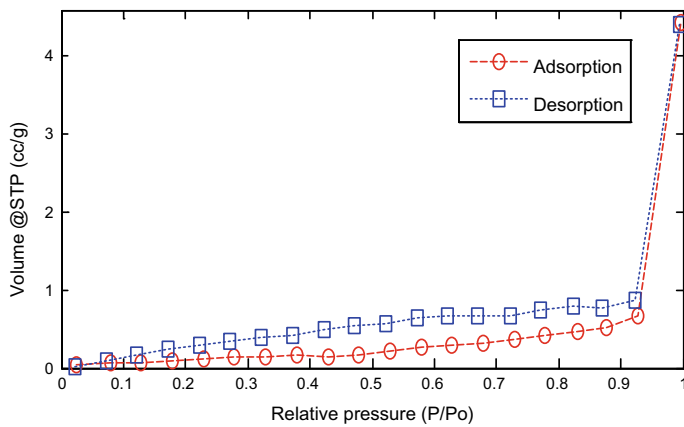


Fig. 5 Adsorption and desorption of AMS biochar

4 Conclusions

The physical and chemical properties of the biochar produced by pyrolysis process from AMS were evaluated, and a comparative study was performed with different biochar. The decomposition of AMS biochar begins at about 300 °C, which indicates that it consists of lignin along with some undecomposed amount of cellulose. The biochar contains higher heating value relative to biomass. Due to the high pH (9.3), the AMS biochar is alkaline in nature and thus it can be used for soil improvement. The biochar of AMS is composed of the compounds which are less oxygenated but more carbonaceous with low O/C atomic ratio when compared with the biomass. Again, the AMS biochar is highly aromatic due to low H/C ratio and helpful for the removal of carbon and resisting the decomposition in soil. The FTIR analysis also shows the functional groups of aromatic carbon due to the peaks with carbon stretching vibration in AMS biochar. The diffractogram of XRD of AMS biochar shows the presence of cellulose with few local crystalline structures. Moreover, the study also reveals the possible existence of SiO₂, CaCO₃, and graphitic carbon in AMS biochar. The surface of AMS biochar is mostly nonporous except few micropores (0.54–1.40 μm). The results of BET analysis indicate the small SSA on AMS biochar which is similar to some other biochar. As further study, the biochar can be produced from the AMS at different temperatures and the detailed study for the various properties can be performed.

Acknowledgements The authors like to acknowledge the Tezpur University for supporting financially in the development of setup for pyrolysis experiments and utilizing different instruments available in various laboratories.

References

1. Yanik J, Kommayer C, Saglam M, Yuksel M (2007) Fast pyrolysis of agricultural waste: characterization of pyrolysis products. *Fuel Process Technol* 88:942–947. <https://doi.org/10.1016/j.fuproc.2007.05.002>
2. Yin R, Liu R, Mei Y, Fei W, Sun X (2013) Characterization of bio-oil and bio-char obtained from sweet sorghum bagasse fast pyrolysis with fractional condensers. *Fuel* 112:96–104. <https://doi.org/10.1016/j.fuel.2013.04.090>
3. Mukherjee A, Lal R (2013) Biochar impacts on soil physical properties and greenhouse gas emissions. *Agronomy* 3:313–339. <https://doi.org/10.3390/agronomy3020313>
4. Kim KH, Kim JY, Cho TS, Choi JW (2012) Influence of pyrolysis temperature on physico-chemical properties of biochar obtained from the fast pyrolysis of pitch pine (*Pinus rigida*). *Bioresour Technol* 118:158–162. <https://doi.org/10.1016/j.biortech.2012.04.094>
5. Brown R (2009) In: Lehman J, Joseph S (eds) *Biochar for environmental management: science and technology*, 2nd edn. Earthscan, London, pp 127–146
6. Beesley L, Moreno-Jiménez E, Gomez-Eyles JL, Harris E, Robinson B, Sizmur T (2011) A review of biochars' potential role in the remediation, revegetation and restoration of contaminated soils. *Environ Pollut* 159:3269–3282. <https://doi.org/10.1016/j.envpol.2011.07.023>

7. Cabrera A, Cox L, Spokas KA, Celis R, Hermosín MC, Cornejo J, Koskinen WC (2011) Comparative sorption and leaching study of the herbicides fluometuron and 4-chloro-2-methylphenoxyacetic acid (MCPA) in a soil amended with biochars and other sorbents. *J Agric Food Chem* 59:12550–12560. <https://doi.org/10.1021/jf202713q>
8. Pituello C, Francioso O, Simonetti G, Pisi A, Toreggiani A, Berti A, Morari F (2015) Characterization of chemical-physical, structural and morphological properties of biochars from biowastes produced at different temperatures. *J Soil Sediment* 15:792–804. <https://doi.org/10.1007/s11368-014-0964-7>
9. Chun Y, Sheng GY, Chiou CT, Xing BS (2004) Compositions and sorptive properties of crop residue-derived chars. *Environ Sci Technol* 38:4649–4655. <https://doi.org/10.1021/es035034w>
10. Tan C, Yaxin Z, Hongtao W, Wenjing L, Zeyu Z, Yuancheng Z, Lulu R (2014) Influence of pyrolysis temperature on characteristics and heavy metal adsorptive performance of biochar derived from municipal sewage sludge. *Bioresour Technol* 164:47–54. <https://doi.org/10.1016/j.biortech.2014.04.048>
11. Lehmann J (2007) Bio-energy in the black. *Front Ecol Environ* 5:381–387. [https://doi.org/10.1890/1540-9295\(2007\)5\[381:BITB\]2.0.CO;2](https://doi.org/10.1890/1540-9295(2007)5[381:BITB]2.0.CO;2)
12. Masiello CA, Druffel ERM (1998) Black carbon in deep-sea sediments. *Science* 280:1911–1913. <https://doi.org/10.1126/science.280.5371.1911>
13. Pessenda LCR, Gouveia SEM, Aravena R (2001) Radiocarbon dating of total soil organic matter and humin fraction and its comparison with ¹⁴C ages of fossil charcoal. *Radiocarbon* 43:595–601. <https://doi.org/10.1017/S0033822200041242>
14. Knoblauch C, Maarifat AA, Pfeiffer EM, Haefele SM (2011) Degradability of black carbon and its impact on trace gas fluxes and carbon turnover in paddy soils. *Soil Bio Biochem* 43:1768–1778. <https://doi.org/10.1016/j.soilbio.2010.07.012>
15. Liu Y, Yang M, Wu Y, Wang H, Chen Y, Wu W (2011) Reducing CH₄ and CO₂ emissions from waterlogged paddy soil with biochar. *J Soils Sediments* 11:930–939. <https://doi.org/10.1007/s11368-011-0376-x>
16. Zhang A, Cui L, Pan G, Li L, Hussain Q, Zhang X, Zheng J, Crowley D (2010) Effect of biochar amendment on yield and methane and nitrous oxide emissions from a rice paddy from Tai Lake plain, China. *Agric Ecosyst Environ* 139:469–475. <https://doi.org/10.1016/j.agee.2010.09.003>
17. Yuan H, Lu T, Zhao D, Huang H, Noriyuki K, Chen Y (2013) Influence of temperature on product distribution and biochar properties by municipal sludge pyrolysis. *J Mater Cycles Waste Manage* 15:357–361. <https://doi.org/10.1007/s10163-013-0126-9>
18. Krull ES, Baldock JA, Skjemstad JD, Smernik RS (2009) Characteristics of biochar: organo-chemical properties. In: Lehman J, Joseph S (eds) *Biochar for environmental management: science and technology*. Earthscan, London, pp 53–66
19. Al-Wabel MI, Al-Omran A, El-Nagar AH, Nadeem M, Usman ARA (2013) Pyrolysis temperature induced changes in characteristics and chemical composition of biochar produced from conocarpus wastes. *Bioresour Technol* 131:374–379. <https://doi.org/10.1016/j.biortech.2012.12.165>
20. Gottipatti R, Mishra S (2013) Preparation of microporous activated carbon from *Aegle marmelos* fruit shell by KOH activation. *Can J Chem Eng* 91:1215–1222. <https://doi.org/10.1002/cjce.21786>
21. Gottipatti R, Mishra S (2016) Preparation of microporous activated carbon from *Aegle marmelos* fruit shell and its application in removal of chromium (VI) from aqueous phase. *J Ind Eng Chem* 36:355–363. <https://doi.org/10.1016/j.jiec.2016.03.005>
22. Ahmad R, Kumar R (2010) Adsorptive removal of congo red dye from aqueous solution using bael shell carbon. *Appl Surf Sci* 257:1628–1633. <https://doi.org/10.1016/j.apsusc.2010.08.111>
23. Roy K, Verma KM, Vikrant K, Goswami M, Sonwani RK, Rai BN, Vellingiri K, Kim K-H, Giri BS, Singh RH (2018) Removal of patent blue (v) dye using indian bael shell biochar: characterization, application and kinetic studies. *Sustainability* 10:2669. <https://doi.org/10.3390/su10082669>
24. Palniandy LK, Yoon LW, Wong WY, Yong S-T, Pang MM (2019) Application of biochar derived from different types of biomass and treatment methods as a fuel source for direct carbon fuel cells. *Energies* 12:2477

25. Bardalai M, Mahanta DK (2016) Characterization of pyrolysis oil derived from bael shell (*Aegle marmelos*). *Environ Eng Res* 21:180–187. <https://doi.org/10.4491/eer.2015.142>
26. Shariff A, Aziz NSM, Abdullah N (2014) Slow pyrolysis of oil palm empty fruit bunches for biochar production and characterisation. *J Phys Sci* 25:97–112
27. Park J, Lee Y, Ryu C, Park YK (2014) Slow pyrolysis of rice straw: analysis of products properties, carbon and energy yields. *Bioresour Technol* 155:63–70. <https://doi.org/10.1016/j.biortech.2013.12.084>
28. Ye L, Zhang J, Zhao J, Luo Z, Tu S, Yin Y (2015) Properties of biochar obtained from pyrolysis of bamboo shoot shell. *J Anal Appl Pyrol* 114:172–178. <https://doi.org/10.1016/j.jaap.2015.05.016>
29. Kong SH, Loh SK, Bachmann RT, Choo YM, Salimon J, Rahim SA (2013) Production and physico-chemical characterization of biochar from palm kernel shell. *AIP Conf Proc* 1571:749–752. <https://doi.org/10.1063/1.4858744>
30. Brewer CE, Schmidt-Rohr K, Satrio JA, Brown RC (2009) Characterization of biochar from fast pyrolysis gasification systems. *Environ Prog Sustain Energy* 28:386–396. <https://doi.org/10.1002/ep.10378>
31. Ronsse F, Hecke SV, Dickinson D, Prins W (2013) Production and characterization of slow pyrolysis biochar: influence of feedstock type and pyrolysis conditions. *GCB Bioenergy* 5:104–115. <https://doi.org/10.1111/gcbb.12018>
32. Angalaeeswari K, Kamaludeen SPB (2017) Production and characterization of coconut shell and mesquite wood biochar. *Int J Chem Stud* 5:442–446
33. Moreira R, dos Reis Orsini R, Vaz JM, Penteado JC, Spinace EV (2017) Production of biochar, bio-oil and synthesis gas from cashew nut shell by slow pyrolysis. *Waste Biomass Valor* 8:217–224. <https://doi.org/10.1007/s12649-016-9569-2>
34. Wu W, Yang M, Feng Q, McGrouther K, Wang H, Lu H, Chen Y (2012) Chemical characterisation of rice straw derived biochar for soil amendment. *Biomass Bioenergy* 47:268–276. <https://doi.org/10.1016/j.biombioe.2012.09.034>
35. Bouqbis L, Daoud S, Koyro H-W, Kammann CI, Ainhout LFZ, Harrouni MC (2016) Biochar from argan shells: production and characterization. *Int J Recycl Org Waste Agric* 5:361–365. <https://doi.org/10.1007/s40093-016-0146-2>
36. Xiao R, Chen X, Wang F, Yu G (2010) Pyrolysis pretreatment of biomass for entrained-flow gasification. *Appl Energy* 87:149–155. <https://doi.org/10.1016/j.apenergy.2009.06.025>
37. Choudhury ND, Chutia RS, Bhaskar T, Katakai R (2014) Pyrolysis of jute dust: effect of reaction parameters and analysis of products. *J Mater Cycles Waste Manage* 16:449–459. <https://doi.org/10.1007/s10163-014-0268-4>
38. Filippis PD, Palma LD, Petrucci E, Scarsella M, Verdone N (2013) Production and characterization of adsorbent materials from sewage sludge by pyrolysis. *Chem Eng Trans* 32:205–210. <https://doi.org/10.3303/CET1332035>
39. Bourke J, Manely-Harris M, Fushimi C, Dowaki K, Nunoura T, Antal MJ Jr (2007) Do all carbonized charcoals have the same chemical structure? 2. A model of the chemical structure of carbonized charcoal. *Ind Eng Chem Res* 46:5954–5967 (2007). <https://doi.org/10.1021/ie070415u>
40. Ghani WAWAK, Mohd A, da Silva G, Bachmann RT, Taufiq-Yap YH, Rashid U, Al-Muhtaseb AH (2013) Biochar production from waste rubber-wood-sawdust and its potential use in C-sequestration: chemical and physical characterisation. *Ind Crop Prod* 44:18–24. <https://doi.org/10.1016/j.indcrop.2012.10.017>
41. Adachi K, Kobayashi M, Takahashi E (1987) Effect of the application of lignin and/or chitin to soil inoculated with *Fusarium oxysporum* on the variation of soil microflora and plant growth. *Soil Sci Plant Nutr* 33:245–259. <https://doi.org/10.1080/00380768.1987.10557570>
42. Keiluweit M, Nico PS, Johnson MG, Kleber M (2010) Dynamic molecular structure of plant biomass-derived black carbon (biochar). *Environ Sci Technol* 44:1247–1253. <https://doi.org/10.1021/es9031419>
43. Özçimen D, Erosy-Meriçbouy A (2010) Characterization of biochar and bio-oil samples obtained from carbonization of various biomass materials. *Renew Energy* 35:1319–1324. <https://doi.org/10.1016/j.renene.2009.11.042>

44. Shabaan A, Se SM, Mitan NMM, Fairuz DM (2013) Characterization of biochar derived from rubber wood sawdust through slow pyrolysis on surface porosities and functional groups. *Procedia Eng* 68:365–371. <https://doi.org/10.1016/j.proeng.2013.12.193>
45. Xiao LP, Sun ZJ, Shi ZJ, Xu F, Sun RC (2011) Impact of hot compressed water pre-treatment on the structural changes of woody biomass for bioethanol production. *BioResources* 6:1576–1598
46. Azargohar R, Dalai AK (2006) Biochar as a precursor of activated carbon. *Appl Biochem Biotech* 131:762–773. <https://doi.org/10.1385/ABAB:131:1:762>
47. Novak JM, Lima I, Xing B, Gaskin JW, Steiner C, Das KC, Ahmedna N, Rehrh D, Watts DW, Busscher WJ, Schomberg H (2009) Characterization of designer biochar produced at different temperatures and their effects on a loamy sand. *Annal Environ Sci* 3:195–206